Applied Mathematics & Information Sciences
An International Journal

http://dx.doi.org/10.18576/amis/200112

Spectral Solutions of the Second-Kind Volterra Integral Equations using Vieta-Fibonacci Operational Matrix

Nasser H. Sweilam[1,*], *Adel Abdelfattah Darwish*[2], *Doaa Gamal Mohamed*[2], *Aliaa Ali Fath-Elbab*[3], *and Adel Abd Elaziz El-Sayed*[4,5]

[1]Department of Mathematics, Faculty of Science, Cairo University, Giza, Egypt
[2]Department of Mathematics, Faculty of Science, Helwan University, Cairo, Egypt
[3]Department of Basic Sciences, Faculty of Industry and Energy Technology, New Cairo Technological University, Cairo, Egypt
[4]Department of Mathematics, College of Education, University of Technology and Applied Sciences, Al-Rustaq 329, Sultanate of Oman
[5]Department of Mathematics, Faculty of Science, Fayoum University, Fayoum 63514, Egypt

Received: 22 Sep. 2025, Revised: 22 Oct. 2025, Accepted: 8 Nov. 2025
Published online: 1 Jan. 2026

Abstract: In this research, we propose a numerical method to compute approximate solutions for second-kind Volterra integral equations (VIEs) and systems of such equations. The VIEs are converted into a system of algebraic equations with undetermined coefficients. To achieve this, we utilized shifted Vieta-Fibonacci polynomials to construct an operational matrix of integration, where the integral operator is defined in the Riemann-Liouville sense. The solutions to second-kind VIEs and their systems are obtained numerically at the collocation points using the Tau method and using the operational matrix constructed for efficient computation.

Keywords: Operational matrix, Riemann-Liouville integral operator, Second-kind Volterra integral equation, Spectral method, Vieta-Fibonacci polynomials.

1 Introduction

Integral equations, defined by an unknown function within an integral, are essential to model phenomena in physics, engineering, biology, and finance [5,17]. They effectively capture systems with memory effects, such as heat conduction, signal processing, and population dynamics, with Volterra integral equations of the second kind being prominent due to their variable integration limits [27]. Volterra integral equations have a wide range of applications in the following fields: Dynamics [19], linear viscoelasticity [15], particle size statistics [7], heat transfer problems [12], viscoelastic stress analysis [3], population dynamics [24], and epidemic study [10]. Numerical methods, including different bases and schemes, provide efficient solutions for these equations in practical applications [13,22].

Spectral methods have grown in popularity over time and are now commonly employed in spatial discretizations of partial differential equations (PDEs) due to their high degree of accuracy [6,28,29]. The global spectral approach might be a favorable option for numerical VIEs because the spectral method is completely capable of solving problems with history dependence. Although these approaches are appropriate for solving Volterra integral equations, we seek to develop an alternative approach here. In fact, there are numerous published approaches and strategies for solving second-kind VIEs [2,9,14,20,21,22,23,25,26]. In numerical techniques, Vieta-Fibonacci polynomials are used to estimate solutions for VIEs and integro-differential equations. These techniques solve these equations using operational matrix approaches [1].

Consider the second-kind Volterra integral equation (VIE) as in the following formula [18]:

$$y(t) + \int_0^t k(t,s)\, y(s)\, ds = f(t). \tag{1}$$

Eq. (1) describes a functional relationship in which the unknown function $y(t)$ is determined by a known kernel function $k(t,s)$, a known forcing function $f(t)$, and

* Corresponding author e-mail: nsweilam@sci.cu.edu.eg

an integral over the interval $[0,t]$. This type of equation arises in various applications, such as physics, engineering, and biological modeling, where the solution $y(t)$ represents a quantity influenced by its historical values weighted by the kernel. The challenge lies in solving for $y(t)$, often requiring numerical methods such as the operational matrix approach based on shifted Vieta-Fibonacci polynomials, which as discussed, offers high accuracy and computational efficiency by transforming the integral equation into a solvable algebraic system.

Moreover, this study highlights the advantages of a proposed method that saves time, reduces errors, and simplifies computations by using an operational matrix-based approach in the Riemann-Liouville integral sense with shifted Vieta-Fibonacci polynomials. The method achieves high accuracy and convergence, as demonstrated by numerical examples in which approximate solutions match exact solutions, regardless of the similarity between provided and unknown functions. Key contributions include the development of this operational matrix-based approach, the proof of its theoretical convergence, and the use of numerical examples to showcase its precision in the addressing of real-world problems requiring highly accurate solutions.

The present paper is organized as follows. After this introduction section 2 explores preliminaries and tools, for example, the Riemann-Liouville integral operator and its properties and the properties of Vieta-Fibonacci polynomials and their shifted variants, along with a description of the proposed solution method. Section 3 details the development of the operational integration matrix based on the Riemann-Liouville sense and its application to numerically solving second-kind Volterra integral equations (VIEs). Section 4 addresses the estimation of errors. Section 5 demonstrates the precision, simplicity, and effectiveness of the proposed method to solve VIEs. The final section provides concluding remarks.

2 Preliminaries and Tools

This section introduces the foundational concepts and methodologies, focusing on the Riemann-Liouville integral operator and its properties, which are crucial for modeling integral calculus problems. It also explores shifted Vieta-Fibonacci polynomials and their role in constructing efficient operational matrices for numerical solutions of Volterra integral equations.

2.1 Riemann-Liouville Integral Operator and Its Properties

In this part, we introduce the fundamental definition and properties of the Riemann-Liouville fractional integral operator, which is a fundamental concept in fractional calculus, used to generalize the notion of integration to non-integer orders.

2.1.1 Main Definition of the Riemann-Liouville Integral Operator

Definition 1.*[16] For a function $f(t)$ defined on an interval $[a,t]$, the Riemann-Liouville fractional integral of order $\alpha > 0$ is defined as:*

$$I_{a+}^{\alpha} f(t) = \frac{1}{\Gamma(\alpha)} \int_a^t (t-s)^{\alpha-1} f(s)\, ds, \quad t > a,$$

where:

- *$\Gamma(\alpha)$ is the Gamma function, which generalizes the factorial for non-integer values ($\Gamma(n) = (n-1)!$ for positive integers n).*
- *α is the order of the fractional integral, typically a positive real number.*
- *a is the lower bound of the integral, often taken as 0 in many applications (i.e., I_{0+}^{α}).*
- *The kernel $(t-s)^{\alpha-1}$ ensures that the integral accounts for fractional behavior, with the singularity at $s = t$ being integrable for $\alpha > 0$.*

When $a = 0$, the operator is often written as:

$$I^{\alpha} f(t) = \frac{1}{\Gamma(\alpha)} \int_0^t (t-s)^{\alpha-1} f(s)\, ds.$$

This operator generalizes standard integration: when $\alpha = 1$, it reduces to the standard integral, that is, $I^1 f(t) = \int_0^t f(s)\, ds$, and for $\alpha = n$ (a positive integer), it corresponds to the n-fold integral.

2.1.2 Some properties of the Riemann-Liouville Integral Operator

The Riemann-Liouville fractional integral operator possesses several important properties that make it useful in solving differential and integral equations, particularly in fractional calculus. Below are the key properties:

- The operator is linear, meaning for any functions $f(t)$ and $g(t)$ and constants c_1, c_2,

$$I^{\alpha}[c_1 f(t) + c_2 g(t)] = c_1 I^{\alpha} f(t) + c_2 I^{\alpha} g(t).$$

This follows from the linearity of the standard integral.

–For $\alpha, \beta > 0$, the Riemann-Liouville integral satisfies:

$$I^{\alpha} I^{\beta} f(t) = I^{\alpha+\beta} f(t).$$

This property shows that applying the fractional integral of order α followed by order β is equivalent to a single fractional integral of order $\alpha+\beta$, provided the integrals are well-defined.

–For a power function $f(t) = t^{\mu}$, where $\mu > -1$, the Riemann-Liouville integral gives:

$$I^{\alpha} t^{\mu} = \frac{\Gamma(\mu+1)}{\Gamma(\mu+\alpha+1)} t^{\mu+\alpha}.$$

This property is useful in analytical solutions and in constructing operational matrices, as it provides an explicit form for polynomial inputs.

–The operator I^{α} is bounded in spaces like $L^{p}[a,b]$ (for $1 \leq p < \infty$) under certain conditions, ensuring stability in numerical applications. For example, in $L^{1}[a,b]$, the operator maps continuous functions to continuous functions, preserving integrability.

–The Riemann-Liouville fractional integral is the left-inverse of the Riemann-Liouville fractional derivative of the same order α. Specifically, for a sufficiently smooth function $f(t)$,

$$D^{\alpha} I^{\alpha} f(t) = f(t),$$

where D^{α} is the Riemann-Liouville fractional derivative. However, the reverse composition $(I^{\alpha} D^{\alpha} f(t))$ may involve additional terms depending on the behavior of $f(t)$ at the boundary $t = a$.

–For integer-order integration, the Riemann-Liouville integral commutes with standard integration, and for $\alpha = 1$, it aligns with classical results, ensuring consistency with traditional calculus.

The Riemann-Liouville integral operator is widely used in fractional differential equations, integral equations (like the second-kind VIE), and modeling phenomena with memory effects, such as viscoelasticity, anomalous diffusion, and control theory. Its ability to handle non-integer orders makes it particularly suited for problems requiring high accuracy in approximating solutions with fractional behavior, as seen in methods using shifted Vieta-Fibonacci polynomials.

2.2 Vieta-Fibonacci polynomials: relevant characteristics and relationships

Definition 2.*[1] Vieta-Fibonacci polynomials $(F_m(t))$, are polynomials of degree $m \in \mathbb{N}_0$ defined using the following formula on the interval $[-2,2]$:*

$$F_m(t) = \frac{\sin(m\phi)}{\sin\phi},$$

where $t = 2\cos\phi$, $\phi \in [0,\pi]$ and $\mathbb{N}_0$ refers to the natural numbers.

These polynomials $(F_m(t))$, are obtained by applying the relation that follows.

$$F_m(t) = tF_{m-1}(t) - F_{m-2}(t), \qquad m = 2,3,\cdots,$$

where the initial values

$$F_0(t) = 0, \quad F_1(t) = 1.$$

Furthermore, the power formula that follows can be used to represent Vieta-Fibonacci polynomials:

$$F_m(t) = \sum_{j=0}^{\lfloor \frac{m-1}{2} \rfloor} (-1)^j \frac{\Gamma(m-j)}{\Gamma(j+1)\Gamma(m-2j)} t^{m-2j-1}, \quad m \in \mathbb{Z}^+, \tag{2}$$

where $\lfloor \frac{m-1}{2} \rfloor$ represents the greatest integer less than or equal to $\frac{m-1}{2}$. Moreover, a family of orthogonal functions constructed by these polynomials, $F_m(t)$, corresponds to the inner product as follows:

$$\langle F_m(t), F_n(t) \rangle = \int_{-2}^{2} \sqrt{4-t^2}\, F_m(t)\, F_n(t)\, dt = \begin{cases} 0, & m \neq n, \\ 2\pi, & m = n. \end{cases} \tag{3}$$

Where $\sqrt{4-t^2}$ is the function that refers to the weight obtained from Vieta-Fibonacci polynomials.

2.3 Shifted Vieta-Fibonacci polynomials

We introduce the conversion and relation between the Vieta-Fibonacci polynomials $F_m(t)$ and their shifted versions $F_m^*(t)$ to utilize them over the domain $[0,1]$ as the following manar.

Definition 3.*[1] The shifted Vieta-Fibonacci polynomials $F_m^*(t)$, of degree m in t on $[0,1]$ are defined as follows:*

$$F_m^*(t) = F_m(4t-2).$$

Additionally, these polynomials can be derived from the recurrence formula:

$$F_m^*(t) = 2(2t-1)F_{m-1}^*(t) - F_{m-2}^*(t), \qquad m = 2,3,\cdots,$$

where the initial values

$$F_0^*(t) = 0, \quad F_1^*(t) = 1.$$

Furthermore, any of the two analytical formulas given below is used to represent the shifted Vieta-Fibonacci polynomials:

$$F_m^*(t) = \sum_{j=0}^{m} (-1)^j \frac{2^{2m-2j-2}\Gamma(2\,m-j)}{\Gamma(j+1)\Gamma(2m-2j)} t^{m-j-1}, \quad m \in \mathbb{Z}^+, \tag{4}$$

or

$$F_m^*(t) = \sum_{j=0}^{m} (-1)^{m-j-1} \frac{2^{2j}\Gamma(m+j+1)}{\Gamma(m-j)\Gamma(2j+2)} t^j, \quad m \in \mathbb{Z}^+. \tag{5}$$

Note that $F_0^*(t)=0$, otherwise, $F_m^*(t)$ can be found in [1]. The orthogonality relation is satisfied by the polynomials $F_m^*(t)$:

$$\langle F_m^*(t),F_n^*(t)\rangle=\int_0^1\sqrt{t-t^2}F_m^*(t)F_n^*(t)\,dt=\begin{cases}0, & m\neq n,\\ \frac{\pi}{8}, & m=n\neq 0.\end{cases} \tag{6}$$

The weight function $\sqrt{t-t^2}$ is derived from the shifted Vieta-Fibonacci polynomials. Now, consider the following shifted Vieta-Fibonacci polynomials as the desired approximate solution:

$$y(t)=\sum_{j=0}^{\infty}c_{j+1}F_{j+1}^*(t), \tag{7}$$

where the function $y(t)\in L_\omega^2[0,1]$ and c_{j+1} are the relevant numerical solution's undetermined coefficients. In Eq. (7), take only $m+1\to\infty$ of the series as follows:

$$y(t)=\sum_{j=0}^{m}c_{j+1}F_{j+1}^*(t)=C^T\psi(t), \tag{8}$$

where $\psi(t)$ is the shifted Vieta-Fibonacci polynomials and C^T refers to the transpose of the vector of the undetermined coefficients.
Using the following relations, the undetermined coefficients vector $C=[c_1,c_2,...,c_{m+1}]^T$ can be obtained:

$$c_{j+1}=\frac{1}{2\pi}\int_{-2}^{2}y\left(\frac{t+2}{4}\right)\sqrt{4-t^2}F_{j+1}(t)dt. \tag{9}$$

or

$$c_{j+1}=\frac{8}{\pi}\int_0^1 y(t)\sqrt{t-t^2}F_{j+1}^*(t)dt. \tag{10}$$

The following matrix form is used to represent the shifted Vieta-Fibonacci polynomials stated in the numerical solution (8).

$$\psi(t)=[F_1^*(t),\,F_2^*(t),\,\cdots,\,F_{m+1}^*(t)]^T. \tag{11}$$

Because these polynomials are power functions, it is possible to define them using the this expression:

$$\psi(t)=BP(t), \tag{12}$$

where $P(t)=[1,t,t^2,...,t^m]^T$, and the matrix B is $(m+1)\times(m+1)$ has the following form:

$$B=\begin{pmatrix} b_{0,0} & 0 & 0 & 0 & \cdots & 0\\ b_{1,0} & b_{1,1} & 0 & 0 & \cdots & 0\\ b_{2,0} & b_{2,1} & b_{2,2} & 0 & \cdots & 0\\ \vdots & \vdots & \vdots & \vdots & \vdots & \vdots\\ b_{m,0} & b_{m,1} & b_{m,2} & \cdots & b_{m,m-1} & b_{m,m}\end{pmatrix}, \tag{13}$$

where the elements of the matrix B are given by:

$$(b_{j,k})_{0\le j,k\le m}=\begin{cases}\frac{(-1)^{j-k-1}(2)^{2k}\Gamma(j+k+1)}{\Gamma(j-k)\Gamma(2k+2)}, & j\ge k,\\ 0, & otherwise.\end{cases} \tag{14}$$

For $m=4$, the matrix in Eq. (13) with the elements in Eq. (14) becomes:

$$B=\begin{pmatrix} 1 & 0 & 0 & 0 & 0\\ -2 & 4 & 0 & 0 & 0\\ 3 & -16 & 16 & 0 & 0\\ -4 & 40 & -96 & 64 & 0\\ 5 & -80 & 336 & -512 & 256\end{pmatrix}, \tag{15}$$

moreover, Eq. (12) can be expressed as follows:

$$P(t)=B^{-1}\psi(t). \tag{16}$$

3 Operational matrix of integration

In this section, the operational matrix of Riemann-Liouville integration will be constructed.

3.1 Operational matrix

The numerical series of the approximated solution in Eq. (1) is examined in this subsection, which focuses on the integration matrix of Riemann-Liouville for the shifted Vieta-Fibonacci polynomials.
Initially, by applying Eq. (8), we get

$$\int_0^t y(s)ds\simeq\int_0^t y_m(s)ds=C^T\int_0^t\psi(s)\,ds. \tag{17}$$

Using the function $\psi(s)$, which is explained in Eq. (12), we have

$$\int_0^t\psi(s)ds=\int_0^t BP(s)\,ds=B\int_0^t[1,s,s^2,\cdots,s^m]^T\,ds. \tag{18}$$

Through the features of the Riemann-Liouville integral operator and its properities [1], Eq. (18) was produced as follows:

$$\begin{aligned}\int_0^t\psi(s)\,ds&=B\int_0^t[1,s,s^2,\cdots,s^m]^T\,ds\\ &=B[t,\frac{1}{2}t^2,\frac{1}{3}t^3,\cdots,\frac{1}{m+1}t^{m+1}]^T\\ &=B\begin{bmatrix}1&0&0&\cdots&0\\0&\frac{1}{2}&0&\cdots&0\\0&0&\frac{1}{3}&\cdots&0\\\vdots&\vdots&\vdots&\vdots&\vdots\\0&0&0&\cdots&\frac{1}{m+1}\end{bmatrix}\begin{bmatrix}t\\t^2\\t^3\\\vdots\\t^{m+1}\end{bmatrix}\\ &=tBUP(t),\end{aligned} \tag{19}$$

where

$$U=\begin{bmatrix}1&0&0&\cdots&0\\0&\frac{1}{2}&0&\cdots&0\\0&0&\frac{1}{3}&\cdots&0\\\vdots&\vdots&\vdots&\vdots&\vdots\\0&0&0&\cdots&\frac{1}{m+1}\end{bmatrix}. \tag{20}$$

Now, using Eq. (16), Eq. (19) can be changed as follows:

$$\int_0^t \psi(s)\,ds = t\,BU\,P(t) = t\,BU\,B^{-1}\,\psi(t). \tag{21}$$

Here, the BUB^{-1} integration's operational matrix is presented. Thus, the integral term in Eq. (1) can be represented as

$$\begin{aligned}\int_0^t y(s)\,ds &\simeq \int_0^t y_m(s)\,ds \\ &\simeq \int_0^t (C^T\psi(s))\,ds \\ &= C^T\int_0^t \psi(s)\,ds = t\,C^T BU\,B^{-1}\,\psi(t).\end{aligned} \tag{22}$$

3.2 Numerical solution for VIE

The following matrix form represents the main problem that was expressed in Eq. (1):

$$t\,C^T BU\,B^{-1}\psi(t) + c(t)\,C^T\psi(t) = f(t), \qquad 0 \le t \le 1. \tag{23}$$

Using the spectral collocation approach and collocation points $t_j = L\frac{(2j+1)}{(2m+2)}$ for
$j = 0,1,...m$, Eq. (23) can be written as:

$$t_j\,C^T BU\,B^{-1}\,\psi(t_j) + c(t_j)\,C^T\psi(t_j) = f(t_j), \qquad 0 \le t_j \le 1. \tag{24}$$

The vector C that is unknown may now be calculated, and the numerical solutions that are assumed in Eq. (8) of the Eq. (1) can be computed.

4 Analysis of convergence

Theorem 4.1. Assume $y(t) \in L_\omega[0,1]$, and $y''(x) \le K$, where K is a constant. Then, shifted Vieta-Fibonacci polynomials is used to describe $y(t)$, the approximate solution series $y_m(t)$ provided in Eq. (8) uniformly approaches the function $y(t)$ $(y_m(t) \to y(t))$ as $(m \to \infty)$. Furthermore, the coefficients in Eq. (10) are limited.i.e.

$$y(t) = \sum_{j=0}^{\infty} c_{j+1} F^*_{j+1}(t), \tag{25}$$

where

$$|c_{j+1}| \le \frac{3K}{2j(j-1)(j+2)(j+3)}, \qquad j > 2. \tag{26}$$

Proof. Assume that Eq. (8) provides an approximation solution, then

$$y_m(t) = \sum_{j=0}^{m} c_{j+1} F^*_{j+1}(t). \tag{27}$$

Since Eq. (9) may be used to derive the unknown coefficients $c_{j+1}, j = 0,2,\cdots,m$, substituting by $4t-2 = 2cos(\phi)$ into it gives the following:

$$c_{j+1} = \frac{2}{\pi}\int_0^\pi y\left(\frac{2+2\cos(\phi)}{4}\right)\sin((j+1)\phi)\,\sin(\phi)\,d\phi. \tag{28}$$

Performing integration by parts twice for Eq. (28), to have

$$c_{j+1} = \frac{1}{8\pi}\int_0^\pi y''(x)\left(\frac{1+\cos(\phi)}{2}\right)\sin(\phi)\,\Phi_j(\phi)\,d\phi, \tag{29}$$

where

$$\begin{aligned}\Phi_j(\phi) = &\frac{1}{j}\left[\frac{\sin_{j-1}(\phi)}{j-1} - \frac{\sin_{j+1}(\phi)}{j+1}\right] \\ &- \frac{1}{j+2}\left[\frac{\sin_{j+1}(\phi)}{j+1} - \frac{\sin_{j+3}(\phi)}{j+3}\right].\end{aligned} \tag{30}$$

Applying the absolute values of the two sides of Eq. (29), then

$$|c_{j+1}| = |\frac{1}{8\pi}\int_0^\pi y''(x)\left(\frac{1+\cos(\phi)}{2}\right)\sin(\phi)\,\Phi_j(\phi)\,d\phi|. \tag{31}$$

Since $y''(x) \le K$ and $|sin\phi| \le 1$ then we claim

$$|c_{j+1}| \le \frac{K}{8\pi}\int_0^\pi |\Phi_j(\phi)|\,d\phi. \tag{32}$$

After performing various mathematical operations and computing the integration, we obtain

$$|c_{j+1}| \le \frac{3K}{2j(j-1)(j+2)(j+3)}, \quad j > 2. \quad \square \tag{33}$$

5 Numerical Examples

This section presents numerical results to verify the accuracy, efficacy, flexibility of use, and simplicity of the presented method. Furthermore, we will discuss the exact solution, the approximate solution (numerical solution), and the absolute error (AE). We calculated the (AE) respectively as follows:

$$AE = |y(t) - y_m(t)|, m \in \mathbb{Z}^+,\ t \in [0,1], \tag{34}$$

In this context, t represents the time variable, while $y(t)$ denotes the exact solution and $y_m(t)$ signifies the numerical solution.

Remark.: In some graphs, the AE values are shown on the vertical axis, while the parameter t is shown on the left statistics horizontal axis. Furthermore, the vertical axis on the *right* side of the Figure represents the exact solutions $y(t)$ and approximate solutions $y_m(t)$ of the solutions, while the horizontal axis represents the values that belong to the parameter t. The others represent the exact and the approximate solutions at different values $m+1$.

Example 1.[22]
Consider the linear VIE of the formula:

$$y(t) = \cos(t) - e^t \sin(t) + \int_0^t e^t y(s)\, ds, \qquad (35)$$

where the exact solution is given by $y(t) = \cos(t)$.

The error norms generated by the recommended method and the method in [22] are compared for different values of $m+1$ in Table1. The AE outcomes for Example 1 for $m = 10$ are shown in Table 1 (second column). The AE is plotted in Figure 1 at $m = 10$, where the analytical and numerical solutions are plotted in Figure 2. It is clear from these outcomes that the recommended approach gives better results than those stated in [22]. Also, The numerical solution is almost similar to the exact solution.

Table 1: Our numerical results of Example 1 at $L = 1$ and $m = 10$.

.

t	Method in [22]	The proposed Method
0	0	2.76446×10^{-13}
0.1	1.54654×10^{-13}	5.77316×10^{-15}
0.2	1.50213×10^{-13}	6.99441×10^{-15}
0.3	1.26765×10^{-12}	6.66134×10^{-15}
0.4	3.47766×10^{-11}	8.99281×10^{-15}
0.5	4.06041×10^{-10}	1.13243×10^{-14}
0.6	3.00573×10^{-9}	1.48769×10^{-14}
0.7	1.63048×10^{-8}	2.00950×10^{-14}
0.8	7.04649×10^{-8}	2.63123×10^{-14}
0.9	2.55996×10^{-7}	4.762857×10^{-14}
1.0	8.10970×10^{-7}	2.23599×10^{-13}

Table 2: our computational the exact solutions and the approximate solutions for Example 1 at $L = 1$ and $m = 5, 10$.

.

t	$y(t)$	$y_5(t)$	$y_{10}(t)$
0	1	1.00000477	1.00000000
0.1	0.99500417	0.99500407	0.99500417
0.2	0.98006658	0.98006649	0.98006658
0.3	0.95533649	0.95533682	0.95533649
0.4	0.92106099	0.92106130	0.92106099
0.5	0.87758256	0.87758282	0.87758256
0.6	0.82533561	0.82533609	0.82533561
0.7	0.76484219	0.76484293	0.76484219
0.8	0.69670671	0.69670735	0.69670671
0.9	0.62160997	0.62161085	0.62160997
1.0	0.54030231	0.54030759	0.54030231

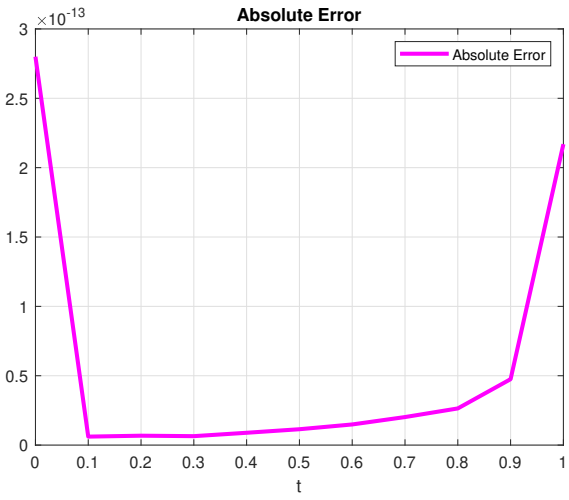

Fig. 1: For Example 1 with $L = 1, m = 10$, the absolute error is plotted

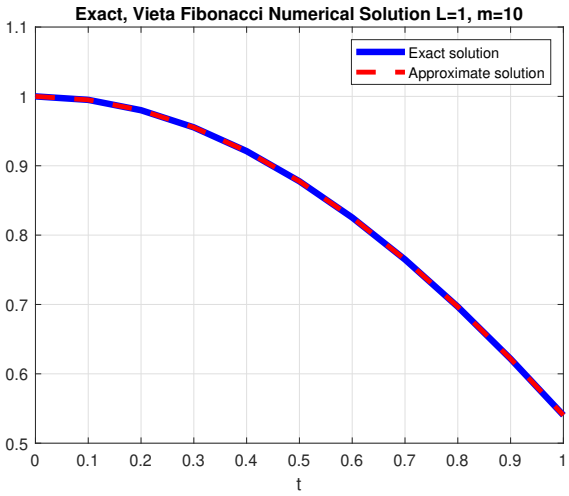

Fig. 2: For Example 1 with $L = 1, m = 10$, the exact and approximate solutions.

Example 2.[11]
Consider the linear VIE

$$y(t) = \cos(t) + \sin(t) + \int_0^t y(s)\, ds, \qquad (36)$$

where the exact solution is given by $y(t) = \cos(t)$.

Table 3: our computational the absolute error for Example 1 at $L = 1$ and $m = 5, 10$.

.

t	$E_5(t)$	$E_{10}(t)$
0	$4.76773214 \times 10^{-6}$	$2.76445533 \times 10^{-13}$
0.1	$9.91092902 \times 10^{-8}$	$5.77315973 \times 10^{-15}$
0.2	$8.93363665 \times 10^{-8}$	$6.99440506 \times 10^{-15}$
0.3	$3.33790384 \times 10^{-7}$	$6.66133815 \times 10^{-15}$
0.4	$3.10741657 \times 10^{-7}$	$8.99280649 \times 10^{-15}$
0.5	$2.56102959 \times 10^{-7}$	$1.13242749 \times 10^{-14}$
0.6	$4.81909138 \times 10^{-7}$	$1.48769885 \times 10^{-14}$
0.7	$7.39739926 \times 10^{-7}$	$2.00950367 \times 10^{-14}$
0.8	$6.38206665 \times 10^{-7}$	$2.63122857 \times 10^{-14}$
0.9	$8.83713696 \times 10^{-7}$	$4.76285678 \times 10^{-14}$
1.0	$5.28415207 \times 10^{-6}$	$2.23598917 \times 10^{-13}$

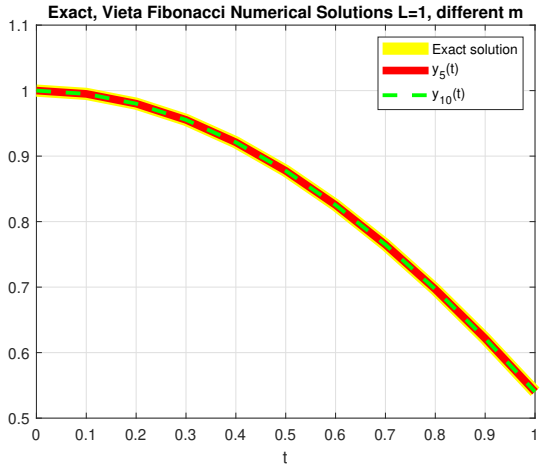

Fig. 3: For Example 1 with $L = 1, m = 5, 10$, the exact and the approximate solutions.

Now, we consider the following System of linear VIEs of the second kind [4]:

$$y_1(t) = f_1(t) + \int_0^t k_{11}(t,s)\,y_1(s)\,ds + \int_0^t k_{12}(t,s)\,y_2(s)\,ds,$$
$$y_2(t) = f_2(t) + \int_0^t k_{21}(t,s)\,y_1(s)\,ds + \int_0^t k_{22}(t,s)\,y_2(s)\,ds, \tag{37}$$

Where $y_1(t)$ and $y_2(t)$ are the unknown functions, $f_1(t), f_2(t)$ and $k_{ij}(t,s), (i,j = 1,2)$ are given functions, and $a_1 \le t \le a_2$.

We propose two numerical examples to verify the accuracy of the provided method for estimating the solution of system given in Equation (37). We have calculated two relative error estimates to demonstrate the

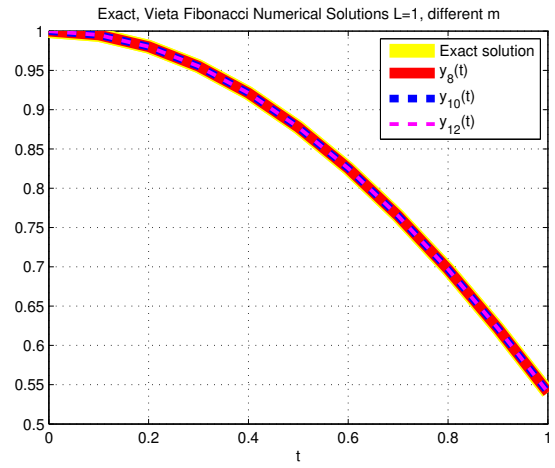

Fig. 4: For Example 2, with the exact and the approximate solutions.

method's accuracy, which are provided by the formulas.

$$E_1 = \frac{1}{1000}\sum_{j=1}^{1000} \langle f(d_j) - (I-K)y_N(d_j)\rangle_m,$$

which calculates the proximity of y_m to the answer of Eq. (37) and

$$E_2 = \sqrt{\frac{\sum_{j=1}^{1000}\langle y_N(d_j - y(d_j))\rangle_m^2}{\sum_{j=1}^{1000}\langle y(d_j)\rangle_m^2}},$$

which approximates the relative error of y_N with respect to t in $L^2((0,1);R^m)$ for a thousand distinct random points, denoted as $d_1, \cdots, d_{1000}$, which are contained in the interval $[0,1]$.

Example 3.[8]
Consider the linear system of VIEs:

$$y_1(t) = t - \frac{t^5}{12} + \int_0^t (t-s)^3 y_1(s)\,ds + \int_0^t (t-s)^2 y_2(s)\,ds,$$
$$y_2(t) = t^2 - \frac{t^6}{20} + \int_0^t (t-s)^4 y_1(s)\,ds + \int_0^t (t-s)^3 y_2(s)\,ds, \tag{38}$$

where the exact solution is given by $y_1(t) = t, y_2(t) = t^2$.

We will use the method described in Section 3 to solve the following problems. we calculate the residual error E_1 and the relative L^2 error E_2 for various polynomial degrees $N = [5, 10, 20, 30, 40, 50]$. Then to make results easier to understand, we will also present a variety of numerical results in Tables and Figures. The results for $N = [5, 10, 20, 30, 40, 50]$, from our method and the one described in [8] are shown in Table 6.

Table 4: Our computational the exact solutions and the approximate solutions for Example 2 at $L = 1$ and $m = 8, 10, 12$.

t	$y(t)$	$y_8(t)$	$y_{10}(t)$	$y_{12}(t)$
0	1	0.999999999803231	1.00000000000023	0.999999999999953
0.1	0.995004165278026	0.99500416529512	0.995004165278014	0.995004165278027
0.2	0.980066577841242	0.980066577841076	0.98006657784124	0.980066577841242
0.3	0.955336489125606	0.955336489128634	0.955336489125603	0.955336489125606
0.4	0.921060994002885	0.92106099400469	0.921060994002883	0.921060994002885
0.5	0.877582561890373	0.877582561892251	0.877582561890371	0.877582561890373
0.6	0.825335614909678	0.82533561491157	0.825335614909677	0.825335614909679
0.7	0.764842187284489	0.764842187285242	0.764842187284487	0.764842187284489
0.8	0.696706709347165	0.696706709351509	0.696706709347162	0.696706709347166
0.9	0.621609968270664	0.621609968254726	0.621609968270675	0.621609968270666
1.0	0.54030230586814	0.540302306126588	0.540302305867811	0.540302305868067

Table 5: Our computational the absolute error for Example 2 at $L = 1$ and $m = 8, 10, 12$.

t	$E_8(t)$	$E_{10}(t)$	$E_{12}(t)$
0	1.96769×10^{-10}	2.33369×10^{-13}	4.72955×10^{-14}
0.1	1.70942×10^{-11}	1.14353×10^{-14}	9.99201×10^{-16}
0.2	1.65867×10^{-13}	1.44329×10^{-15}	4.44089×10^{-16}
0.3	3.02758×10^{-12}	2.55351×10^{-15}	3.33067×10^{-16}
0.4	1.80445×10^{-12}	2.10942×10^{-15}	2.22045×10^{-16}
0.5	1.87805×10^{-12}	1.88738×10^{-15}	3.33067×10^{-16}
0.6	1.89204×10^{-12}	1.7763×10^{-15}	3.33067×10^{-16}
0.7	7.53508×10^{-13}	1.11022×10^{-15}	1.11022×10^{-16}
0.8	4.34397×10^{-12}	3.10862×10^{-15}	3.33067×10^{-16}
0.9	1.59386×10^{-11}	1.03251×10^{-14}	1.33227×10^{-15}
1.0	2.58448×10^{-10}	3.28626×10^{-13}	7.26086×10^{-14}

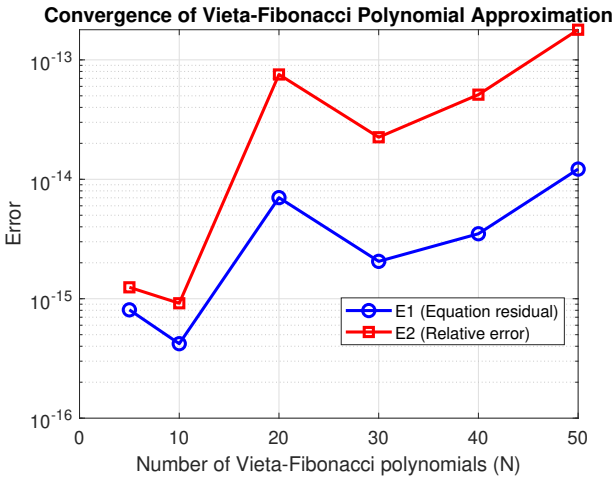

Fig. 5: For Example 3 with $N = [5, 10, 20, 30, 40, 50]$, the two relative errors.

The residual equation E_1 and the relative L^2 error E_2 produced by the suggested technique and the method in [8] are compared at distinct values of $N = [5, 10, 20, 30, 40, 50]$ in Table 6. The two relative errors are plotted at $N = [5, 10, 20, 30, 40, 50]$, as shown in Figure 5. It is clear from these results that the proposed strategy provides better outcomes than those presented in [8]. Furthermore, the analytical and numerical solutions are almost the same.

Example 4.[4] Consider the linear system of VIEs:

$$y_1(t) = 1 - \frac{t^2}{2} + \int_0^t y_1(s)\,ds + \int_0^t se^s y_2(s)\,ds,$$
$$y_2(t) = 1 + \frac{t^2}{2} + \int_0^t -se^{-s} y_1(s)\,ds - \int_0^t y_2(s)\,ds. \qquad (39)$$

Where the exact solution is given by $y_1(t) = e^t, y_2(t) = e^{-t}$.

6 Conclusion

To numerically solve linear second-kind Volterra integral equations (VIEs), we developed a general formulation for the operational matrix of integration based on the Riemann-Liouville operator. This study explores Vieta-Fibonacci polynomials and their shifted variants, leveraging their properties to derive approximate solutions for VIEs by constructing an operational integration matrix that transforms these equations into a system of algebraic equations for efficient numerical resolution. Error analysis is provided to validate the method's reliability, and several numerical examples illustrate its accuracy, effectiveness, and applicability, demonstrating excellent results even as the problem's domain expands. The Vieta-Fibonacci polynomials offer a robust alternative basis for VIE solutions, achieving high precision with fewer collocation points, with all computations performed using MATLAB. Future

Table 6: Our computational relative error estimations for Example 3 at $N = [5, 10, 20, 30, 40, 50]$ provided by the presented method are compared with the relative error estimations provided by the method in [8].

N	Method in [8]		The proposed Method	
	E_1	E_2	E_1	E_2
5	2.1868×10^{-2}	3.1058×10^{-2}	1.0034×10^{-15}	1.4931×10^{-15}
10	3.6034×10^{-3}	4.8048×10^{-3}	4.7050×10^{-16}	1.1387×10^{-15}
20	6.2683×10^{-4}	8.2990×10^{-4}	7.0655×10^{-15}	7.6174×10^{-14}
30	2.0727×10^{-4}	3.0254×10^{-4}	1.7023×10^{-15}	2.0690×10^{-14}
40	1.0215×10^{-4}	1.2509×10^{-4}	3.6885×10^{-15}	5.2964×10^{-14}
50	6.4520×10^{-5}	9.2824×10^{-5}	1.2227×10^{-14}	1.8064×10^{-13}

Table 7: Our computational relative error estimations for Example 4 at $N = [5, 10, 20, 30, 40, 50]$ provided by the presented method.

N	E_1	E_2
5	2.1562×10^{-5}	2.6134×10^{-5}
10	1.2923×10^{-12}	2.8204×10^{-12}
20	1.8993×10^{-14}	6.4466×10^{-14}
30	3.1693×10^{-15}	8.6632×10^{-15}
40	1.0629×10^{-14}	4.4541×10^{-14}
50	5.3813×10^{-15}	2.2925×10^{-14}

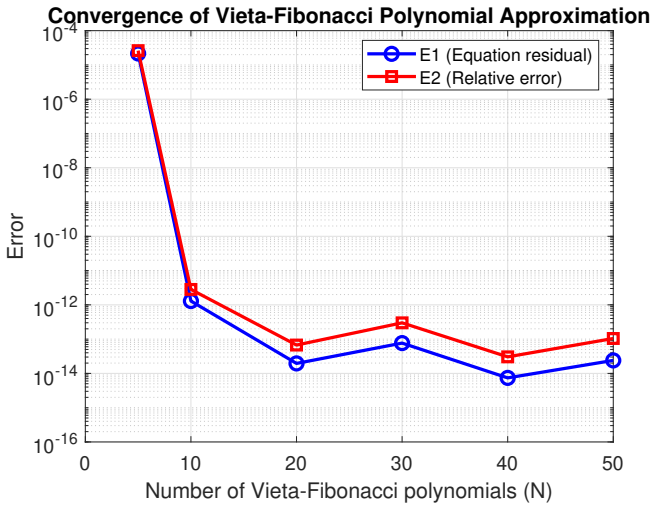

Fig. 6: For Example 4 with $N = [5, 10, 20, 30, 40, 50]$, the two relative errors.

extensions of this operational matrix could address fractional-order partial differential equations, and the proposed method shows promise for solving mathematical models with enhanced accuracy and reduced computational effort.

References

[1] P. Agarwal, A. A. El-Sayed, and J. Tariboon, Vieta-Fibonacci operational matrices for spectral solutions of variable-order fractional integro-differential equations, Journal of Computational and Applied Mathematics, 382, 113063, (2021). https://doi.org/10.1016/j.cam.2020.113063

[2] S. Aggarwal, N. Sharma, and R. Chauhan, Solution of linear Volterra integral equations of second kind using Mohand transform, International Journal of Research in Advent Technology, 6(11), 3098-3102, (2018).

[3] R. S. Anderssen, A. R. Davies, and F. R. De Hoog, On the Volterra integral equation relating creep and relaxation, Inverse Problems 24, 3, 035009, (2008). https://doi.org//0266-5611/24/3/035009

[4] V. Balakumar and K. Murugesan, Numerical solution of systems of linear Volterra integral equations using block-pulse functions, Malaya Journal of Matematik, S (1), 77-84, (2013).

[5] H. Brunner, Volterra integral equations: an introduction to theory and applications, Cambridge University Press, 30, (2017). https://doi.org/10.1017/9781316162491

[6] C. Canuto, A. Quarteroni, M. Y. Hussaini, T. A. Zang Jr, Spectral methods: evolution to complex geometries and applications to fluid dynamics, Berlin, Heidelberg: Springer Berlin Heidelberg, (2007).

[7] P. L. Goldsmith, The calculation of true particle size distributions from the sizes observed in a thin slice, British Journal of Applied Physics 18, 813, (1967). https://doi.org/10.1088/0508-3443/18/6/317

[8] P. González-Rodelas, M. Pasadas, A. Kouibia, B. Mustafa, Numerical Solution of Linear Volterra Integral Equation Systems of Second Kind by Radial Basis Functions, Mathematics, 10(2), 223, (2022). https://doi.org/10.3390/math10020223

[9] J. Izadian, S. Salahshour, S. Soheil, numerical method for solving Volterra and Fredholm integral equations using homotopy analysis method, AWER Proc. Inf. Technol, Comput. Sci, 1, 406-411, (2012).

[10] R. Katani, Numerical solution of a system of Volterra integral equations in application to the avian human influenza epidemic model, Iranian Journal of Numerical Analysis and Optimization 12, 1, 37-53, (2022). https://doi.org/10.22067/ijnao.2021.69416.1021

[11] A. P. Lukonde, D. D. Demir, H. Emadifar, M. Khademi, and H. Azizi, Pell?Lucas polynomial method for Volterra integral equations of the second kind, Afrika Matematika, 34(3), 52, (2023). https://doi.org/10.1007/s13370-023-01096-y

[12] W. R. Mann and F. Wolf, Heat transfer between solids and gases under nonlinear boundary conditions, Quarterly of Applied Mathematics, 9(2), 163-184, (1951). https://doi.org/10.1090/qam/42596

[13] M. Montazer, R. Ezzati, and M. Fallahpour, Numerical solution of Linear Volterra Integral Equations Using Non-Uniform Haar Wavelets, Kragujevac Journal of Mathematics, 47(4), 599-612, (2023). https://doi.org/10.46793/KgJMat2304.599M

[14] M. M. Mustafa and I. N. Ghanim, Numerical solution of linear Volterra-Fredholm integral equations using Lagrange polynomials, Mathematical Theory and Modeling, 4(5), 137-146, (2014).

[15] M. Ortiz, Linear viscoelasticity: Mechanics, analysis and approximation, arXiv preprint arXiv:2509.03485, (2025). https://doi.org/10.48550/arXiv.2509.03485

[16] I. Podlubny, Fractional differential equations: an introduction to fractional derivatives, fractional differential equations, to methods of their solution and some of their applications. Academic press 1999.

[17] A. D.Polyanin and A. V. Manzhirov, Handbook of Integral Equations, CRC Press LLC, (1998).

[18] F. A. A. M. Salameh. Analytical and numerical solutions of volterra integral equation of the second kind, M.Sc. thesis, An-Nagah National University, Nablus, Palestine, (2014).

[19] F. Zakęś and P. śniady, Application of Volterra integral equations in dynamics of multispan uniform continuous beams subjected to a moving load, Shock and Vibration 2016, 1, 4070627, (2016). https://doi.org/10.1155/2016/4070627

[20] E. S. Shoukralla, M. Kamel, and M. A. Markos. A new computational method for solving weakly singular Fredholm integral equations of the first kind, 13th International Conference on Computer Engineering and Systems (ICCES), Cairo, Egypt, (2018). https://doi.org/10.1109/ICCES.2018.8639387

[21] E. S. Shoukralla and M. A. Markos, The economized monic Chebyshev polynomials for solving weakly singular Fredholm integral equations of the first kind, Asian-European Journal of Mathematics, 13(01), 2050030, (2020). https://doi.org/10.1142/S1793557120500308

[22] E. S. Shoukralla and B. M. Ahmed, Numerical solutions of Volterra integral equations of the second kind using Lagrange interpolation via the Vandermonde matrix, J. Phys. Conf. Ser. 1447 (2020), Paper ID 012003. https://doi.org/10.1088/1742-6596/1447/1/012003

[23] E. S. Shoukralla, A. A. Hasan, R. A. Gomaa, A. Yehia, Solution of Volterra Integral Equations of the Second Kind with Weakly Singular Kernels Using Legendre Polynomials, Journal of Advanced Research in Applied Sciences and Engineering Technology 53, Issue 1, 32-43, (2025). https://doi.org/10.37934/araset.53.1.3243

[24] K. E. Swick, A nonlinear model for human population dynamics, SIAM Journal on Applied Mathematics, 40(2), 266-278, (1981). https://doi.org/10.1137/0140023

[25] G. Uma, V. Prabhakar, S. Hariharan, Numerical integration using hybrid of block-pulse functions and Lagrange polynomial, International Journal of Pure and Applied mathematics, 106(5), 33-44, (2016).

[26] W. Wang, A mechanical algorithm for solving the Volterra integral equation, Applied Mathematics and Computation, 172(2), 1323-1341, (2006). https://doi.org/10.1016/j.amc.2005.02.056

[27] A.-M. Wazwaz, Linear and Nonlinear Integral Equations: Methods and Applications, Springer, Berlin, Heidelberg, (2011).

[28] Z. Xiao-Yong, L. Yan, Generalized Laguerre pseudospectral method based Laguerre interpolation, Applied Mathematics and Computation, 219(5), 2545-2563, (2012). https://doi.org/10.1016/j.amc.2012.08.090

[29] X. Y. Zhang, Mixed spherical harmonic-generalized Laguerre spectral method for the Navier?Stokes equations, Journal of Numerical Mathematics, 21(3), 231-264, (2013).

Nasser H. Sweilam is professor of numerical analysis at the Department of Mathematics, Faculty of Science, Cairo University. He was a channel system Ph.D. student between Cairo University, Egypt, and TU-Munich, Germany. He received his Ph.D. in Optimal Control of Variational Inequalities, the Dam Problem. He was the Head of the Department of Mathematics, Faculty of Science, Cairo University, May 2012-2018. He is referee and editor of several international journals, in the frame of pure and applied Mathematics. His main research interests are numerical analysis, optimal control of differential equations, fractional and variable order calculus, bio-informatics and cluster computing and ill-posed problems.

Adel Darwish is professor Emeritus of Mathematics, Faculty of Science, Helwan University- Academic Advisor to the Egyptian Chinese University in Cairo - Former Cultural Advisor and Director of the Egyptian Cultural Center in Baku, Embassy of the Arab Republic of Egypt in Azerbaijan- Ambassador of Culture.

Doaa Gamal Mohamed is Lecturer of pure mathematics, Faculty of Science, Helwan University. Her research interests are numerical analysis, optimal control of differential equations, fractional and variable calculus and biomathematics. She has published research articles in reputed international journals of mathematical science.

Aliaa Ali Fath-Elbab is a Teaching Assistant of Mathematics, Faculty of Industry and Energy Technology, New Cairo Technological University in Cairo. She graduated from the Faculty of Science, Menoufia University. She is currently a master's student at the Faculty of Science, Helwan University.

A. A. El-Sayed is an Assistant Professor of Numerical Analysis. He obtained his Ph.D. in Pure Mathematics from Fayoum University in 2016. He has published numerous scientific papers in the fields of numerical analysis, spectral methods, special functions, and fractional analysis. Dr. El-Sayed has contributed to peer-reviewing many research articles for reputable international journals and serves as a reviewer for several prestigious scientific publications.